





# Widen the Resonance at Ultra-High Energies: Novel Probes of Neutrino Self-interactions in the High-Mass Regime

Pedro A. N. Machado <sup>1\*</sup>, Isaac R. Wang <sup>1†</sup>, Xun-Jie Xu <sup>2‡</sup>, Bei Zhou <sup>1,3§</sup>

<sup>1</sup> *Theory Division, Fermi National Accelerator Laboratory, Illinois 60510, USA*

<sup>2</sup> *Institute of High Energy Physics, Chinese Academy of Sciences, Beijing 100049, China*

<sup>3</sup> *Kavli Institute for Cosmological Physics, University of Chicago, Chicago, Illinois 60637, USA*

## Abstract

Neutrino self-interaction beyond the Standard Model is well motivated by the nonzero masses of neutrinos, which are the only known particles guaranteed to have new physics. Cosmic messengers, especially neutrinos, play a central role in probing new physics, as they provide experimental conditions far beyond the reach of laboratories and serve as the link between laboratory fundamental-physics discoveries and their roles in the Universe, where many new physics motivations originate. In this work, we propose a novel probe of neutrino self-interactions through ultra-high-energy neutrinos scattering off the cosmic neutrino background when the lightest neutrino species remains relativistic today. This allows us to “*Widen the Resonance*” of such scattering [1]. Meanwhile, we also provide a semi-analytic framework for cosmogenic UHE neutrino production, avoiding computationally intensive simulations and yielding results precise enough for BSM studies. The widened resonance enables future ultrahigh-energy neutrino telescopes, in particular GRAND, to probe mediator masses from MeV to GeV, reaching couplings down to  $g \sim 10^{-3}$ —up to two orders of magnitude beyond current bounds. Our results enhance the discovery potential of  $\nu$ SI in the high-mass regime, potentially offering crucial insights into the connections between the neutrino sector and dark sector.

---

\*pmachado@fnal.gov

†isaacw@fnal.gov

‡xuxj@ihep.ac.cn

§beizhou@fnal.gov

---

# Contents

<b>1</b>	<b>Introduction</b>	<b>1</b>
<b>2</b>	<b>Neutrino self-interactions</b>	<b>3</b>
2.1	Lagrangian . . . . .	3
2.2	Resonant absorption and mean-free-path estimate . . . . .	4
2.3	Boltzmann equation . . . . .	5
<b>3</b>	<b>Modeling cosmogenic UHE neutrino production</b>	<b>7</b>
<b>4</b>	<b>Neutrino Propagation</b>	<b>10</b>
<b>5</b>	<b>Detection, likelihood analysis, and results</b>	<b>11</b>
<b>6</b>	<b>Conclusion</b>	<b>14</b>
<b>A</b>	<b>More details for Section 3—modeling cosmogenic UHE neutrino production</b>	<b>15</b>

---

## 1 Introduction

Neutrinos are the only known particles that guarantee connections to new physics, as their nonzero masses are beyond the Standard Model (BSM). Explaining their masses typically introduces new mediators that naturally lead to BSM neutrino self-interactions ( $\nu$ SI), which can be much stronger than those in the Standard Model (SM) mediated by  $Z$  bosons <sup>1</sup>. The possible existence of  $\nu$ SI could also provide a portal to other well-motivated new physics, such as dark matter and matter-antimatter asymmetry. Therefore,  $\nu$ SI provides a promising avenue to discover new physics.  $\nu$ SI have rich phenomena in particle physics, astrophysics, and cosmology. As a result,  $\nu$ SI has been a subject of growing interest in recent years, using various ways to probe  $\nu$ SI [1–33]; see also Ref. [34] for a recent review.

Besides that, cosmic messengers, especially neutrinos, play a central role in probing new physics, providing energies, baselines, and other properties way beyond the reach of laboratory neutrinos (e.g., Refs [1, 32, 35, 36]). While laboratory searches for new physics provide a controlled, well-understood setup, many new-physics motivations arise from questions related to cosmology and astrophysics, such as the nature of dark matter. Thus, cosmic and astrophysical neutrinos provide a natural link between laboratory fundamental-physics discoveries and their potential roles in the Universe. For  $\nu$ SI, astrophysical neutrinos provide a powerful test because they can scatter off the cosmic neutrino background (CNB) during propagation through  $\nu$ SI [1, 15, 16, 18, 19, 22, 31, 32], which would significantly reduce the flux or distort their spectra, both effects being detectable at neutrino telescopes.

In more detail,  $\nu$ SI are well motivated from the perspective of model building [37–49]. They could be mediated by, e.g., a new light scalar or vector particle with mass  $m_\phi$  and coupling  $g$  to neutrinos. The effective four-Fermi interaction strength is  $G_X \equiv g^2/m_\phi^2$ , currently constrained to

---

<sup>1</sup>Hereafter,  $\nu$ SI solely denotes BSM neutrino self-interactions

$G_X \lesssim 10^2 - 10^9 G_F$  from laboratory experiments [3–5], supernova dynamics [9–13], cosmology [25–28], and astrophysical neutrino propagation [15–23], depending on the mass of the mediator. Such new self-interactions could render the Universe partially opaque to ultra-high-energy (UHE) neutrinos through scattering on the CNB. Of particular importance is resonant scattering via  $\nu\nu_{\text{CNB}} \rightarrow \phi \rightarrow \nu\nu$ , where the  $s$ -channel mediator production satisfies  $s = m_\phi^2$ . For non-relativistic CNB with neutrino mass  $m_\nu \gg T_{\text{CNB}} \approx 1.9 \text{ K} = 0.16 \text{ meV}$ , the resonance condition gives  $s \simeq 2E_\nu m_\nu$ , or

$$E_\nu^{\text{res}} \simeq \frac{m_\phi^2}{2m_\nu}. \quad (1)$$

To probe, e.g.,  $m_\phi \sim 100 \text{ MeV}$  with  $m_\nu \sim 0.05 \text{ eV}$ , requires neutrinos with  $E_\nu \sim 100 \text{ PeV}$ , i.e., at high-energy (HE; TeV–PeV) or ultrahigh-energy (UHE; PeV–EeV) energies [35]. Several studies have investigated this mechanism as a probe of  $\nu\text{SI}$  with IceCube and future IceCube-Gen2 and the Giant Radio Array for Neutrino Detection (GRAND) [15–18, 32, 50, 51].

While the above studies assume a fully non-relativistic CNB, this assumption is not required by neutrino oscillation data, which constrain only  $\sum m_\nu \gtrsim 0.06 \text{ eV}$ , allowing one mass eigenstate to satisfy  $m_\nu < T_{\text{CNB}}$ . Certain neutrino mass models strictly predict a massless neutrino that satisfies this scenario, for example, simple loop-level mechanisms [52] or minimal seesaws with only two right-handed standard model singlets [53, 54]. Besides, recent cosmological measurements from DESI suggest  $\sum m_\nu$  may be close to the minimum value allowed by oscillations [55], making a relativistic CNB component increasingly plausible.

For a relativistic neutrino species, the momentum distribution is thermal rather than monochromatic, with energies ranging from  $\sim 0.1T_{\text{CNB}}$  to  $\sim 10T_{\text{CNB}}$ . This thermal distribution significantly alters the resonance phenomenology. The resonance condition for relativistic scattering is  $s = 2E_\nu E_{\text{CNB}}(1 - \cos\theta)$ , where  $\theta$  is the scattering angle and  $E_\nu$  is the energy of the incoming UHE neutrino. Since both  $E_{\text{CNB}}$  and  $\theta$  vary, many different combinations of  $(E_\nu, E_{\text{CNB}}, \cos\theta)$  can satisfy  $s = m_\phi^2$ . This widens the resonance over one order of magnitude in  $E_\nu$ , in contrast to the narrow absorption feature expected for a non-relativistic CNB. This widening was recently demonstrated for the diffuse supernova neutrino background at MeV energies [1], which enables sensitivity to sub-keV mediators and surpasses the existing constraints by orders of magnitude.

The concept of “widening the resonance” is more general than astrophysical neutrinos scattering off relativistic CNB. It straightforwardly applies to situations in which both initial states follow continuum energy distributions; for example, other astrophysical neutrinos like the diffuse supernova neutrino background [56] or terrestrial neutrinos. Thus, we encourage relevant future work in a broader range of topics.

In this work, we extend the “widening the resonance” concept to UHE neutrinos. The widened resonance provides key advantages: it affects a larger range of the observable UHE neutrino spectra, yielding greater statistical power and overcoming the potential energy-resolution limitation. We show that GRAND can probe mediator masses in the MeV–GeV scales with couplings down to  $g \sim 10^{-3}$ , corresponding to  $G_X \sim 10G_F$ . This leads to improvements of up to two orders of magnitude over current constraints, as well as significant gains with respect to the non-relativistic CNB case. In addition, to model cosmogenic UHE neutrino production, we develop a semi-analytic framework that significantly simplifies computation compared to computationally intensive simulations and can be useful for future studies.

This paper is organized as follows. In Sec. 2, we define the general Lagrangian for a scalar-mediated  $\nu\text{SI}$ , with a dedicated description of the flavor structure and the Boltzmann equation that governs neutrino propagation. In Sec. 3, we provide a semi-analytic framework to model the cosmogenic UHE neutrino production. Then, we illustrate the spectral distortion on UHE neutrinos due to  $\nu\text{SI}$  in Sec. 4. The necessary technical details for solving the Boltzmann equations are also

discussed. In Sec. 5, we derive our projected sensitivities from detecting these spectral distortions in GRAND with likelihood analyses. We also discuss our results. We conclude in Sec. 6.

## 2 Neutrino self-interactions

In this section, we demonstrate how  $\nu$ SI attenuates the UHE neutrino propagation. We begin by setting up the  $\nu$ SI model considered in this work. We then illustrate the impact of the relativistic CNB neutrinos by calculating the absorption rate of the propagating UHE neutrinos. This allows us to estimate the sensitivity based on the mean free path. Finally, we derive the Boltzmann equation necessary to solve for the UHE neutrino propagation.

### 2.1 Lagrangian

Neutrino self-interactions typically involve a new mediator that couples exclusively or predominantly to neutrinos. In the simplest setup, the mediator is assumed to be a real scalar,  $\phi$ , with the following mass and interaction terms:

$$\mathcal{L} \supset -\frac{1}{2}m_\phi^2\phi^2 + \frac{1}{2}(g_{\alpha\beta}\phi\nu_\alpha\nu_\beta + \text{h.c.}), \quad (2)$$

where  $m_\phi$  denotes the mediator mass,  $\nu_{\alpha,\beta}$  with  $\alpha, \beta \in (e, \mu, \tau)$  are SM left-handed neutrinos, and  $g_{\alpha\beta}$  is the coupling matrix in the flavor eigenbasis. Throughout, we assume that neutrinos are Majorana fermions so that right-handed neutrinos are not involved in this work. To clarify potential confusions, here we note that  $\nu$ 's in Eq. (2) denote two-component Weyl spinors, instead of four-component Majorana spinors  $\chi_M \equiv (\nu, \nu^\dagger)^T$ . When performing a unitary transformation  $\nu \rightarrow U\nu$ , where  $U$  is a unitary matrix, the Majorana spinors cannot transform in the same way as the Weyl spinor unless  $U$  is real.

To calculate the scattering between the propagating UHE neutrino and the CNB neutrino, it is convenient to transform the coupling matrix into the mass eigenbasis. This is achieved by taking  $U$  to be the PMNS matrix, under which the neutrino fields are transformed as:

$$\begin{pmatrix} \nu_e \\ \nu_\mu \\ \nu_\tau \end{pmatrix} = U \begin{pmatrix} \nu_1 \\ \nu_2 \\ \nu_3 \end{pmatrix}, \quad (3)$$

where  $\nu_1, \nu_2$ , and  $\nu_3$  are the three neutrino mass eigenstates. Correspondingly, the  $g_{\alpha\beta}\nu_\alpha\nu_\beta$  term is transformed to  $g_{ij}\nu_i\nu_j$  with  $i, j \in (1, 2, 3)$ . The transformation of the coupling matrices is given by

$$g_{ij} = \sum_{\alpha,\beta} g_{\alpha\beta} U_{\alpha i} U_{\beta j}. \quad (4)$$

Here, both  $g_{\alpha\beta}$  and  $g_{ij}$  are symmetric matrices. Throughout this work, we use  $g_{ij}$  to represent the coupling matrix in the mass eigenbasis and  $g_{\alpha\beta}$  in the gauge eigenbasis.

Since in general  $U^T U \neq I$  where  $I$  is the identity matrix (due to the CP phases in  $U$ ),  $g_{ij}$  is not necessarily diagonal even if one assumes a flavor-universal coupling, i.e.  $g_{\alpha\beta} = g_{\text{univ}} I$ . Specifically, if one neglects the Majorana phases in  $U$ , the coupling matrix in the mass eigenbasis can be explicitly calculated as

$$g_{ij} \approx g \begin{pmatrix} 1 & 0 & -2ic_{12}s_{13}s_\delta \\ 0 & 1 & -2is_{12}s_{13}s_\delta \\ -2ic_{12}s_{13}s_\delta & -2is_{12}s_{13}s_\delta & 1 \end{pmatrix} + \mathcal{O}(s_{13}^2), \quad (5)$$

where  $c_{ij}$  ( $s_{ij}$ ) is  $\cos\theta_{ij}$  ( $\sin\theta_{ij}$ ) with  $\theta_{ij}$  being the mixing angle between mass eigenstates  $i$  and  $j$ . The  $\delta$  is the complex, CP-violating phase. One can notice the existence of the off-diagonal elements, though suppressed by the smallness of  $s_{13}$ . Taking the limit of  $\delta \rightarrow 0$  leads Eq. (5) to  $I$ . Throughout this work, we fix the PMNS mixing parameters at their best fit values in NuFIT5.3 [57, 58],  $\theta_{12} = 33.7^\circ$ ,  $\theta_{13} = 8.54^\circ$ ,  $\theta_{23} = 49.0^\circ$ , and  $\delta_{\text{CP}} = 197^\circ$ , assuming normal mass ordering. And for simplicity, we set all Majorana phases to zero.

Before ending this subsection, we would like to comment on possible models that can give rise to the interactions in Eq. (2). Since  $\phi$  is assumed to be exclusively coupled to neutrinos but not charge leptons, one might be concerned about the issue of gauge invariance in model building. However, given that the electroweak  $SU(2)$  symmetry is broken at low energies, a new light mediator arising from BSM theories does not necessarily have to couple equally to neutrinos and their  $SU(2)$  partners in their low-energy effective theory. One of the most well-known examples is the Majoron model [37–39], in which the Majoron is predominantly coupled to neutrinos while its coupling to charged leptons is loop suppressed, roughly by a factor of  $G_{\text{F}} m_\nu m_\ell / (16\pi^2)$  [37]. With separate seesaw mechanisms between different neutrino flavors, a large  $\nu_\tau$ -philic coupling can be generated [3]. Other models that introduce light mediators through the right-handed neutrino portal typically share the same feature [46–48]. Therefore, from the model-building point of view, it is plausible that some hidden sector mediators may couple to neutrinos much more strongly than to other SM particles.

## 2.2 Resonant absorption and mean-free-path estimate

In this subsection, we present a qualitative description of the UHE neutrino spectrum distortion by estimating the mean free path of UHE neutrinos, taking into account the dominant effect, i.e., the widened resonance. A quantitative study that accounts for all the above effects requires solving the Boltzmann equation, which is presented in the next subsection.

When a UHE neutrino of energy  $E_\nu$  propagates through CNB, it could scatter off a CNB neutrino via  $\nu\nu \rightarrow \phi \rightarrow \nu\nu$ . If the  $s$ -channel resonance is reached,  $\phi$  can be produced on-shell, absorbing the incoming UHE neutrino. The cross section at the resonance is

$$\sigma_{ij}^{(\text{res})} \simeq \pi g_{ij}^2 \delta(s - m_\phi^2), \quad (6)$$

where  $s = 2E_\nu E_{\text{CNB}}(1 - \cos\theta)$  is the Mandelstam variable with  $E_{\text{CNB}}$  the energy of the CNB neutrino, and  $\theta$  the angle between the two initial-state neutrinos. Later,  $\phi$  decays back into two neutrinos, each with roughly half of the energy of the incoming neutrino. For the relativistic CNB, there is a wide range for  $E_{\text{CNB}}$  and  $\cos\theta$  to satisfy the resonance condition at  $s = m_\phi^2$ , allowing for a large range of UHE neutrino energies to resonantly scatter off the CNB neutrinos. This constitutes the key point of our idea: the “widening the resonance” from scattering the relativistic CNB<sup>2</sup>.

By integrating Eq. (6) with the thermal distribution of CNB neutrinos, we obtain the absorption rate, which is defined as the probability of absorption per unit time (or equivalently, per unit propagation length for UHE neutrinos). The absorption rate for the  $i$ -th mass eigenstate is [1]

$$\Gamma_{\text{abs},i} \simeq \frac{g_{i1}^2 m_\phi^2 T}{16\pi E_\nu^2} \exp\left[-\frac{m_\phi^2}{4TE_\nu}\right], \quad (7)$$

where  $T$  is the temperature of the CNB. Note that within the assumed normal mass ordering only  $\nu_1$  contribute to the absorption rate. If we had assumed inverted ordering,  $\nu_3$  would take that role.

---

<sup>2</sup>Note that Eq. (6) could also be applied to a non-relativistic CNB, but it is impractical to calculate the  $\nu\nu \rightarrow \phi$  resonant scattering directly due to its extremely narrow resonance. Instead, one often incorporates it into the Breit-Wigner formula for the  $s$ -channel  $\nu\nu \rightarrow \nu\nu$  scattering—see, e.g., Eq. (25) in Ref. [59].

Equation (7) tells us that UHE neutrinos can be effectively absorbed by the CNB during propagation if their energies are in an appropriate range: if  $E_\nu \ll m_\phi^2/4T$ , the absorption rate is suppressed by the exponential factor  $\exp(-m_\phi^2/4TE_\nu)$ ; if  $E_\nu$  is too large, it is suppressed by  $E_\nu^2$  in the denominator. The most effective absorptions occur around the energy that maximizes  $\Gamma_{\text{abs}}$ ,

$$E_\nu^{\text{peak}} = \frac{m_\phi^2}{8T}. \quad (8)$$

The corresponding absorption rate at this maximum is  $\Gamma_{\text{abs}} = 4g^2T^3/(\pi e^2 m_\phi^2)$ . The smooth exponential form of Eq. (7) leads to a widened resonance peak: the width of the resonance for  $E_\nu$  is given by  $\Delta E_\nu \sim m_\phi^2/T_{\text{CNB}} \simeq 10^9$  GeV for  $m_\phi \simeq 100$  MeV, while the Breit-Wigner resonance width for a non-relativistic CNB is  $\Delta E_\nu \sim m_\phi \Gamma_\phi/m_\nu \simeq 1$  GeV for the same  $m_\phi$  and  $m_\nu \simeq 0.1$  eV.

Whether our Universe is opaque to UHE neutrinos under  $\nu$ SI and relativistic CNB can then be estimated by the mean free path at small  $z$ , with the interaction rate given by Eq. (7). For UHE neutrinos moving at the speed of light, the mean free path is  $L = 1/\Gamma_{\text{abs}}$  and the specific value is given as

$$L \simeq 3.2 \text{ Gpc} \left( \frac{10^{-3}}{|g_{i1}|} \right)^2 \left( \frac{E_\nu}{2 \text{ EeV}} \right)^2 \left( \frac{50 \text{ MeV}}{m_\phi} \right)^2 e^\lambda, \quad (9)$$

where  $\lambda \equiv m_\phi^2/4TE_\nu$  is around 1.9 for  $E_\nu$  and  $m_\phi$  varying around their respective benchmark values in Eq. (9). The mean free path is to be compared with the radius of the Universe  $R_{\text{Univ}} = 14.2$  Gpc. For  $E_\nu = 2$  EeV,  $m_\phi = 50$  MeV, and  $|g_{i1}| = 10^{-3}$ , the mean free path  $L \simeq 21.6$  Gpc is comparable to  $R_{\text{Univ}}$ , implying that the CNB would be half-opaque/half-transparent to UHE neutrinos at this energy. Consequently, a significant portion of such UHE neutrinos would be absorbed during propagation, leading to observable effects in the UHE energy spectrum and flavor composition. Specifically, when  $E_\nu$  reaches  $E_\nu^{\text{peak}}$ , the absorption becomes the most significant and the mean free path  $L$  reaches its minimum

$$L_{\text{min}} \equiv \min_{E_\nu} L \simeq 22 \text{ Gpc} \left( \frac{10^{-3}}{g_{i1}} \right)^2 \left( \frac{50 \text{ MeV}}{m_\phi} \right)^2. \quad (10)$$

Figure 1 shows the sensitivity estimated from Eq.(9) in the blue shaded region. For each point, we scan  $E_\nu \in [0.1, 100]$  EeV and take the minimum value of  $L$  in this range. The boundary of the shaded region corresponds to  $L_{\text{min}} \leq 10$  Gpc obtained in this way. For clarity, we also plot several black dashed lines indicating  $L_{\text{min}} = 0.01, 0.1, 1.0$ , and  $14.2$  Gpc for UHE neutrinos whose energies hit the resonance peak, where  $L_{\text{min}}$  is computed using Eq. (10). Above each line, UHE neutrinos with  $E_\nu$  near  $E_\nu^{\text{peak}}$  undergo strong absorption and are expected to be absorbed within the corresponding interaction length  $L_{\text{min}}$ . Consequently, if such neutrinos are produced at a distance  $D \gg L_{\text{min}}$ , the flux at  $E_\nu = E_\nu^{\text{peak}}$  would be exponentially suppressed by a factor  $\exp(-D/L_{\text{min}})$ .

### 2.3 Boltzmann equation

To carefully study the impact of  $\nu$ SI on UHE neutrino propagation in a quantitative way, we employ the following Boltzmann equation:

$$\left( \frac{\partial}{\partial t} - H p \frac{\partial}{\partial p} \right) F = - \begin{bmatrix} \Gamma_{\nu(3 \times 3)}^- & \\ & \Gamma_\phi^- \end{bmatrix} F + \begin{bmatrix} \Gamma_{\nu(3 \times 1)}^+ & \\ & \Gamma_\phi^+ \end{bmatrix} + \begin{bmatrix} S_{\nu(3 \times 1)} \\ 0 \end{bmatrix}, \quad (11)$$

$$F \equiv (f_{\nu_1}, f_{\nu_2}, f_{\nu_3}, f_\phi)^T,$$

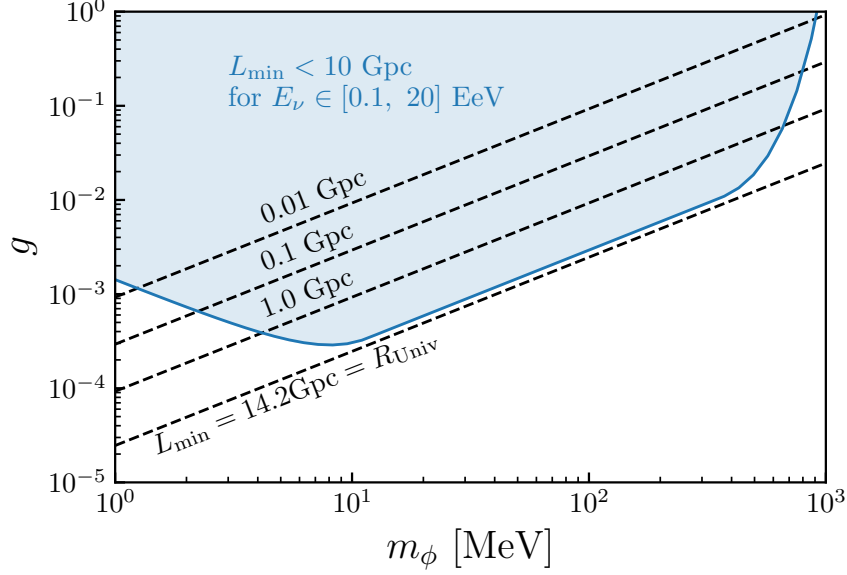


Figure 1: Mean-free-path estimate of the  $\nu$ SI strength relevant to UHE neutrino propagation. The **black dashed lines** are obtained using Eq. (10), and the **blue region** is obtained by further imposing a finite range of  $E_\nu$ .

where  $f_X$  with  $X \in \{\nu_1, \nu_2, \nu_3, \phi\}$  denotes the phase space distribution of particle  $X$ ,  $\Gamma_\nu^\pm$  and  $\Gamma_\phi^\pm$  are production and depletion rates of  $\nu$  and  $\phi$  via scattering or decay processes, and  $S_\nu$  is the astrophysical source term, which will be elaborated in Sec. 3. We use  $+$  ( $-$ ) to denote the creation (depletion) rate of a certain particle species. The subscripts  $(3 \times 3)$  and  $(3 \times 1)$  indicate the shapes of matrices and will be omitted in what follows. The Hubble parameter  $H$  receives contributions mainly from matter and dark energy for  $1 \leq 1+z \lesssim 10$ . Hence it can be determined by

$$H \approx H_0 \sqrt{\Omega_\Lambda + \Omega_m a^{-3}}, \quad (12)$$

where  $H_0 \approx 67.36$  km/s/Mpc is the present value of  $H$ ,  $\Omega_m \approx 0.315$  and  $\Omega_\Lambda \approx 0.685$  denote the matter and dark energy density parameters [60], and  $a \equiv 1/(1+z)$  is the scale factor of the Universe.

The production and depletion rates  $\Gamma_\nu^\pm$  and  $\Gamma_\phi^\pm$ , also known as the collision terms, receive both resonant and non-resonant contributions. The resonant contribution ( $\propto g_{i1}^2$ ) is significantly higher than the non-resonant ones ( $\propto g_{ij}^4$ ) when the  $s$ -channel resonance is kinematically accessible. Under the assumption that the lightest species in the CNB is relativistic, an UHE astrophysical neutrino, if sufficiently energetic, can always find a relativistic CNB neutrino with appropriate momentum to scatter resonantly. Therefore, in this work, we only focus on the resonant contribution. By generalizing the corresponding collision terms previously derived in Ref. [1] to three flavors, we



obtain

$$\Gamma_{\nu}^{-} = G_{3 \times 3} \frac{m_{\phi}^2 T}{16\pi E_{\nu}^2} \exp \left[ -\frac{m_{\phi}^2}{4TE_{\nu}} \right], \quad (13)$$

$$\Gamma_{\nu}^{+} = G_{3 \times 1} \frac{2m_{\phi}^2}{16\pi E_{\nu}^2} \int_{E_{\phi}^{\min}}^{\infty} dE_{\phi} f_{\phi}, \quad (14)$$

$$\Gamma_{\phi}^{+} = \sum_i (G_{3 \times 3})_{ii} \frac{m_{\phi}^2}{16\pi E_{\phi} p_{\phi}} \int_{E_{\nu}^{-}}^{E_{\nu}^{+}} dE_{\nu} f_{\nu_i} \exp \left[ -\frac{E_{\phi} - p_{\nu}}{T} \right], \quad (15)$$

$$\Gamma_{\phi}^{-} = G_{1 \times 1} \frac{m_{\phi}^2}{16\pi E_{\phi}}, \quad (16)$$

where  $T \approx 1.9 \text{ K} \cdot (1+z)$  is the CNB temperature (varying significantly at high  $z$ ),  $E_X$  and  $p_X$  denote the energy and momentum of  $X \in \{\nu, \phi\}$ ,  $E_{\phi}^{\min} = \frac{m_{\phi}^2}{4E_{\nu}} + E_{\nu}$ , and  $E_{\nu}^{\mp} = (E_{\phi} \mp p_{\phi})/2$ . The matrices  $G_{3 \times 3}$ ,  $G_{3 \times 1}$ , and  $G_{1 \times 1}$  are defined for convenience as follows

$$G_{3 \times 3} \equiv \begin{pmatrix} |g_{11}|^2 & 0 & 0 \\ 0 & |g_{21}|^2 & 0 \\ 0 & 0 & |g_{31}|^2 \end{pmatrix}, \quad G_{3 \times 1} \equiv \begin{pmatrix} \sum_i |g_{1i}|^2 \\ \sum_i |g_{2i}|^2 \\ \sum_i |g_{3i}|^2 \end{pmatrix}, \quad G_{1 \times 1} \equiv \sum_{ij} |g_{ij}|^2. \quad (17)$$

It is noteworthy that if the three components of  $\Gamma_{\nu}^{+}$  are summed up, the total creation rate of all neutrino flavors is independent of the PMNS mixing:

$$\sum_j \Gamma_{\nu,j}^{+} \propto \sum_{ij} |g_{ij}|^2 = \text{Tr}(g_{ij}^{\dagger} g_{ij}) = \text{Tr}(g_{\alpha\beta}^{\dagger} g_{\alpha\beta}) = \sum_{\alpha\beta} |g_{\alpha\beta}|^2. \quad (18)$$

### 3 Modeling cosmogenic UHE neutrino production

In this section, we provide a semi-analytic framework for cosmogenic UHE neutrino production, avoiding computationally intensive simulations and precise enough for phenomenology studies. The cosmogenic UHE neutrino production acts as the source term,  $\mathcal{S}_{\nu}$ , in Eq. (11), which is a crucial ingredient in our work. We provide a pedagogical description of the semi-analytic approach, which is useful for phenomenological work beyond the scope of this paper.

In general, UHE neutrinos have two main origins (see Refs. [35, 61] for recent reviews). The first is cosmogenic, from UHE cosmic rays scattering off the cosmic microwave background (CMB) at temperatures  $\sim 10^{-4} \text{ eV}$ , or the extragalactic background light at  $\sim 1 \text{ eV}$ . The second is directly from astrophysical objects, like certain types of active galactic nuclei or supernovae [62, 63]. The neutrino flux from the second origin is highly model-dependent and uncertain, so we ignore this component as a conservative choice. Note that if the flux is comparable to or higher than that from the cosmogenic origin, UHE neutrinos will be an even more powerful tool for testing new physics (this is especially motivated by the recent KM3NeT detection of the  $\sim 200 \text{ PeV}$  neutrino event, which implies a UHE neutrino flux much higher than typical cosmogenic fluxes [64, 65]).

The cosmogenic UHE neutrino production can be written as

$$\mathcal{S}_{\nu}(E_{\nu}, a) = \frac{2\pi^2}{E_{\nu}^2} \frac{dN_{\nu}}{dE_{\nu}}(E_{\nu}, a) \text{SE}(a) \frac{1}{a^3}, \quad (19)$$

where  $a \equiv 1/(1+z)$  is the scale factor and the time variable here.



The source evolution factor  $SE(a)$  in Eq. (19) can be parametrized as [32, 66]

$$SE(z) = \begin{cases} (1+z)^m, & z < 1 \\ 2^m, & 1 \leq z < 4 \\ 2^m \left(\frac{1+z}{5}\right)^{-3.5}, & 4 \leq z < 7. \end{cases} \quad (20)$$

The value of  $m$  depends on the source type; for example, redshift evolutions of the star-formation rate, gamma-ray burst, and active galactic nuclei typically follow  $m = 3$  [67], whereas BL Lacertae objects exhibit an overall flat evolution, i.e.,  $m \simeq 0$  [68–71].

The energy spectra of the produced UHE neutrinos,  $dN_\nu/dE_\nu$  in Eq. (19), is determined by the following processes [66, 72–77]. We ignore the interactions between cosmic rays and the extragalactic background light, as its density is much lower than that of the CMB. We also treat the UHECRs as all protons, as the uncertainties due to the chemical compositions can be absorbed into the source-evolution uncertainties governed by  $m$  [32].

- **Photopion production:** Protons with energies  $E_p \gtrsim 55$  EeV can create  $\Delta^+$  resonantly that then decays into a pion and a nucleon, i.e.  $p\gamma \rightarrow \Delta^+ \rightarrow \pi^+ n / \pi^0 p$ , with the branching ratio into  $\pi^+ n$  being 1/3. The  $\pi^+$  then decays into neutrinos. This is the dominant contribution to the cosmogenic UHE neutrino flux.
- **Neutron  $\beta$  decay:** The neutrons produced together with  $\pi^+$  from the above process can decay into  $\bar{\nu}_e$ . This is suppressed by more than 2 orders of magnitude compared to photopion production for  $E_\nu > 0.1$  EeV, because the produced neutrinos have only  $10^{-3}$ – $10^{-4}$  of the UHECR energies (as a comparison, the photopion produced neutrinos have  $\sim 0.05$ ). Thus, it is negligible in the energy range considered in this work.
- **Multiple scattering:** Nucleons produced in the initial interactions can also scatter off CMB photons to generate UHE neutrinos, and the subsequently produced nucleons further contribute in the same way. However, the steeply falling spectra of UHECRs suppress these additional contributions.
- **Pair production:** Protons can lose energy due to pair production from scattering the CMB, i.e.,  $p\gamma \rightarrow pe^-e^+$ . The scattering length is  $\sim 1$  Gpc, significantly larger than that of photopion production (about 100 Mpc). Consequently, the energy loss from pair production is negligible [72, 78, 79].
- **Adiabatic energy loss:** Protons lose energy due to the expansion of the Universe. This is also negligible for the energy range considered in our work.

Including all the processes above requires computationally intensive simulations [32, 66, 73]. Instead, we provide a simplified, semi-analytic framework for calculating  $dN_\nu/dE_\nu$  and show that the results are consistent with those from simulations within theoretical uncertainties, as follows.

From the above discussion, we focus on the dominant process for cosmogenic UHE neutrino production, i.e., photopion production. To calculate the neutrino spectra at production,  $dN_\nu/dE_\nu(E_\nu, a)$ , of this process, we adopt the widely used semi-analytic framework given in Ref. [72]. For a given neutrino species  $i$ ,

$$\frac{dN_{\nu,i}}{dE_\nu}(E_\nu, z) = \int f_p(E_p) f_{\text{CMB}}(\epsilon, z) \Psi_i(\eta, x) \frac{dE_p}{E_p} d\epsilon, \quad (21)$$

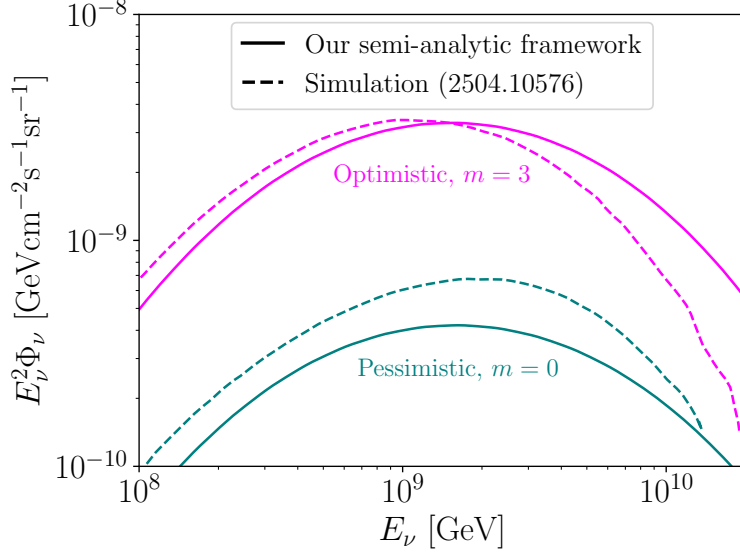


Figure 2: Neutrino energy spectrum without  $\nu$ SI calculated using our semi-analytic framework, which is consistent with the result from computationally intensive simulations [32, 77] within the theoretical uncertainty characterized by the difference between the two solid or dashed lines. We show the results for our benchmark cases,  $\Gamma = 2.5$ ,  $E_{\text{max}} = 250$  EeV, with  $m = 0$  and 3 being optimistic and pessimistic scenarios, respectively; the same conclusion applies to results for other parameter values.

where  $x \equiv E_{\nu,i}/E_p$  is the energy ratio between the produced neutrino and the proton,  $\eta \equiv 4\epsilon E_p/m_p^2$  is the center of mass (CoM) energy of the proton-photon scattering, normalized by  $m_p$ . The integration is over the proton energy  $E_p$  and the CMB photon energy  $\epsilon$ . The crucial quantity is  $\Psi(\eta, x)$ , which is the neutrino spectrum per proton-photon interaction. We refer the readers to Appendix A for the details about the form of  $\Psi$  and the range of  $\eta$ . This quantity is convoluted with the CMB photon spectrum at redshift  $z$ ,  $f_{\text{CMB}}(\epsilon, z)$ , and the UHE cosmic-ray proton energy density,  $f_p(E_p)$ , which is directly related to their spectrum [80, 81]

$$\frac{dN_\nu}{dE_p} = N_p E_p^{-\Gamma} \exp\left(-\frac{E_p}{E_p^{\text{max}}}\right), \quad (22)$$

where  $N_p$  is the normalization factor to match the local ( $z \cong 0$ ) measurements [80, 81] around 40 EeV [32, 82], as UHECRs can only travel distances of  $\sim 100$  Mpc. In addition,  $\Gamma \in [2, 3]$  is the spectral index and  $E_p^{\text{max}}$  is the cut-off energy.

With these fitted functions, one can perform a numerical integration for Eq. (21). The results, together with the source evolution factor in Eq. (20), are then used to calculate the neutrino production in Eq. (19). Finally, as the neutrino oscillation length is much smaller than any astrophysical scales here and neutrino mixing angles are large, we expect an approximately flavor-independent flux of neutrinos soon after they are produced, i.e., all the flavors have the same flux.

Fig. 2 shows the neutrino energy spectrum without  $\nu$ SI calculated by our semi-analytic framework and, as a comparison, the result from simulations [32]. The difference is much smaller than the uncertainties, which validates our semi-analytic framework.

## 4 Neutrino Propagation

With the collision and source terms constructed, we can solve the Boltzmann equation numerically. Although in the original Boltzmann equation,  $F$  is a function of  $t$  and  $p$ , in practice, we solve the equation using the variable transformation from  $(t, p)$  to  $(a, \tilde{p})$  where  $\tilde{p} \equiv ap$  is the comoving momentum. Such a variable transformation not only removes the  $H p \partial_p$  term in Eq. (11), but also improves the numerical stability and performance of the code, since the comoving momentum is unchanged during propagation in the expanding Universe in the absence of collisions. For the technical details of the implementation, we refer to the appendix of Ref. [1].

By discretizing the comoving momentum space into 200 bins for each particle species, we solve the  $200 \times 4$  coupled differential equations using the `solve_ivp` solver in `scipy` with the BDF method. From the obtained values of  $f_{\nu,i}$ , it is straightforward to calculate the present-day UHE neutrino flux  $\Phi_{\nu,i}$ , which is related to  $f_{\nu,i}$  by

$$\Phi_{\nu,i} = \frac{E_\nu^2}{2\pi^2} f_{\nu,i}, \quad (i = 1, 2, 3). \quad (23)$$

Note that during propagation, the UHE neutrino fluxes are calculated in the mass basis, while their detection involves fluxes in the flavor basis,  $\Phi_{\nu,\alpha}$ , which are related to  $\Phi_{\nu,i}$  by

$$\Phi_{\nu,\alpha} = \sum_i |U_{\alpha i}|^2 \Phi_{\nu,i}. \quad (24)$$

We investigate the following two representative scenarios of  $\nu$ SI

- Flavor-universal coupling:  $g_{\alpha\beta} = g_{\text{univ}} I$ , where  $I$  is the identity matrix and  $g_{\text{univ}}$  denotes the coupling strength. This scenario leads to an approximately diagonal coupling matrix in the mass basis—see Eq. (5).
- $\nu_\tau$ -philic coupling:  $g_{\alpha\beta} = \text{diag}(0, 0, g_{\tau\tau})$ . This scenario is the least constrained by laboratory bounds [3], while we specifically emphasize the importance of future sensitivity explored in this work.

In Fig. 3, we present the UHE neutrino spectra obtained by solving the Boltzmann equation for the two scenarios defined above. The black dashed curves denote free propagation (with the source parameters  $E_{\text{max}} = 250$  EeV,  $\Gamma = 2.5$ , and  $m = 3$ ) while the solid curves include the effect of  $\nu$ SI with  $g_{\tau\tau}(g_{\text{univ}}) = 2 \times 10^{-3}$ ,  $m_\phi = 50$  MeV. In general, all spectra exhibit absorption at high energies and regeneration at low energies. In the  $\nu_\tau$ -philic scenario (the left panel), these effects are similar for all three flavors. In contrast, in the flavor-universal scenario (the right panel),  $\nu_e$  shows a more prominent absorption feature, while  $\nu_{\mu,\tau}$  spectra display stronger regenerations. In both scenarios, the absorption feature appears as a smooth, widened dip rather than a deep, narrow resonance peak, as a result of the widened resonance.

The key difference arises from the nearly diagonal structure of the coupling matrix in the mass basis for the universal coupling case—see Eq. (5). In the limit of  $s_{13} \rightarrow 0$ , Eq. (5) becomes exactly diagonal, implying that only  $\nu_1$  can be absorbed by the relativistic CNB. If all  $\nu_1$  particles are fully absorbed without regeneration of new particles, the resulting UHE flux would contain only  $\nu_2$  and  $\nu_3$ , leading to the following flavor composition:

$$\Phi_{\nu,e} : \Phi_{\nu,\mu} : \Phi_{\nu,\tau} \approx s_{12}^2 : 1 - c_{23}^2 s_{12}^2 : 1 - s_{23}^2 s_{12}^2 \approx \frac{1}{3} : \frac{5}{6} : \frac{5}{6}, \quad (25)$$

since  $s_{12}^2 \approx 1/3$  and  $c_{23}^2 \approx s_{23}^2 \approx 1/2$ . This ratio shows that the  $\nu_e$  flux is strongly suppressed while the reductions in  $\Phi_{\nu,\mu}$  and  $\Phi_{\nu,\tau}$  are relatively modest, assuming no neutrino regeneration and

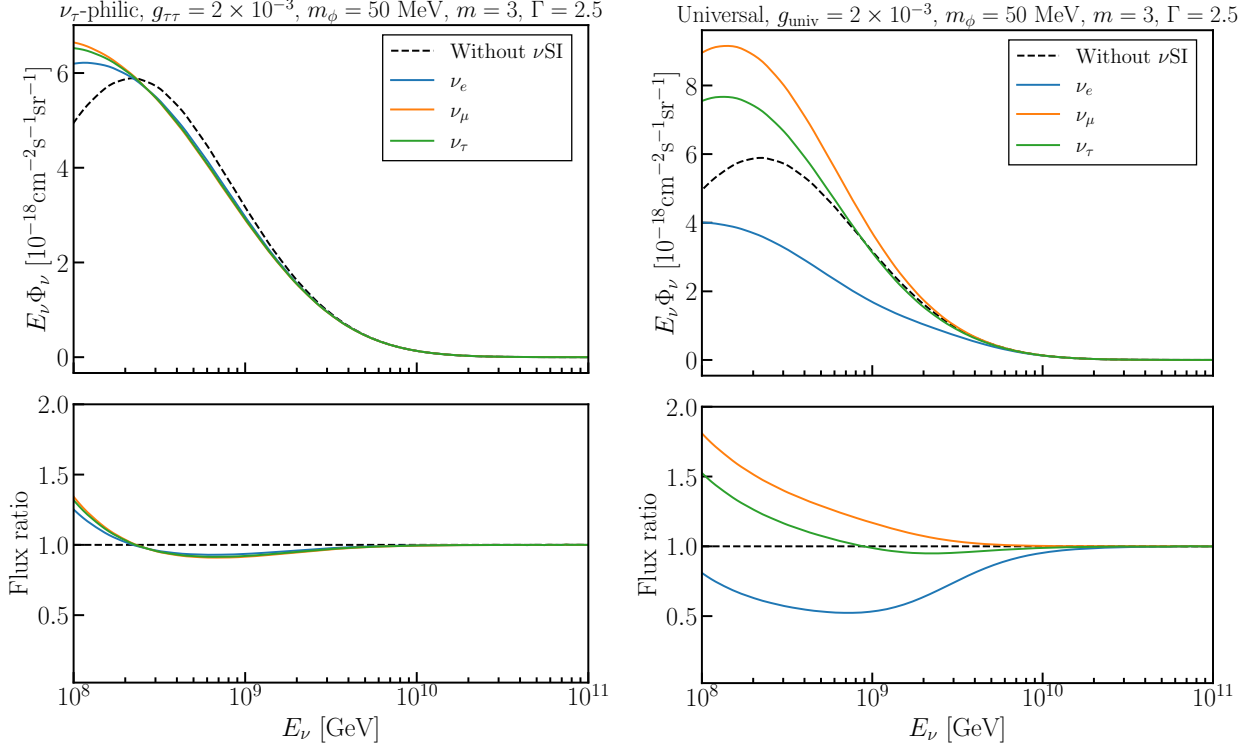


Figure 3: UHE neutrino fluxes modified by  $\nu$ SI. The left and right panels assume flavor universal and  $\nu_\tau$ -philic couplings, respectively. The upper panels present the flux spectrum, whereas the lower panels show the ratio of the modified flux to the standard one with free propagation.

a perfectly diagonal  $g_{ij}$ . We then include the effect of neutrino regeneration from  $\phi$  decay. Since the decay rate into each flavor is the same, the regenerated UHE neutrinos compensate all three flavor fluxes equally (though at lower energies). Combining both absorption and regeneration effects, the  $\nu_e$  flux remains dominated by absorption, while the final  $\nu_\mu$  and  $\nu_\tau$  fluxes become larger than their original values due to the regenerated neutrinos produced from absorbed  $\nu_e$ . In comparison, in the  $\nu_\tau$ -philic scenario, the absorption effect is much more evenly distributed among  $\nu_1$ ,  $\nu_2$ , and  $\nu_3$ . Using the latest global fit central values of the PMNS mixing parameters, we obtain

$$g_{ij} \approx g_{\tau\tau} \begin{pmatrix} 0.25 & 0.29 & 0.32 \\ 0.29 & 0.33 & 0.37 \\ 0.32 & 0.37 & 0.42 \end{pmatrix}, \quad (26)$$

which shows that the absorption effect on  $\nu_3$  is only slightly stronger than on  $\nu_2$  and  $\nu_1$ . Neglecting this small difference, all three mass eigenstates experience nearly the same degree of absorption. As a result, the three curves for  $\nu_e$ ,  $\nu_\mu$ , and  $\nu_\tau$  in the right panel of Fig. 3 lie very close to one another.

## 5 Detection, likelihood analysis, and results

For the UHE neutrino detection, we focus here on the Giant Radio Array for Neutrino Detection (GRAND) [83]. GRAND is one of the most representative experiments among those employing a promising experimental strategy that relies on the observation of extensive air showers (EAS) from the decay of Earth-emergent tau leptons induced by tau-neutrino charged-current interactions [35].

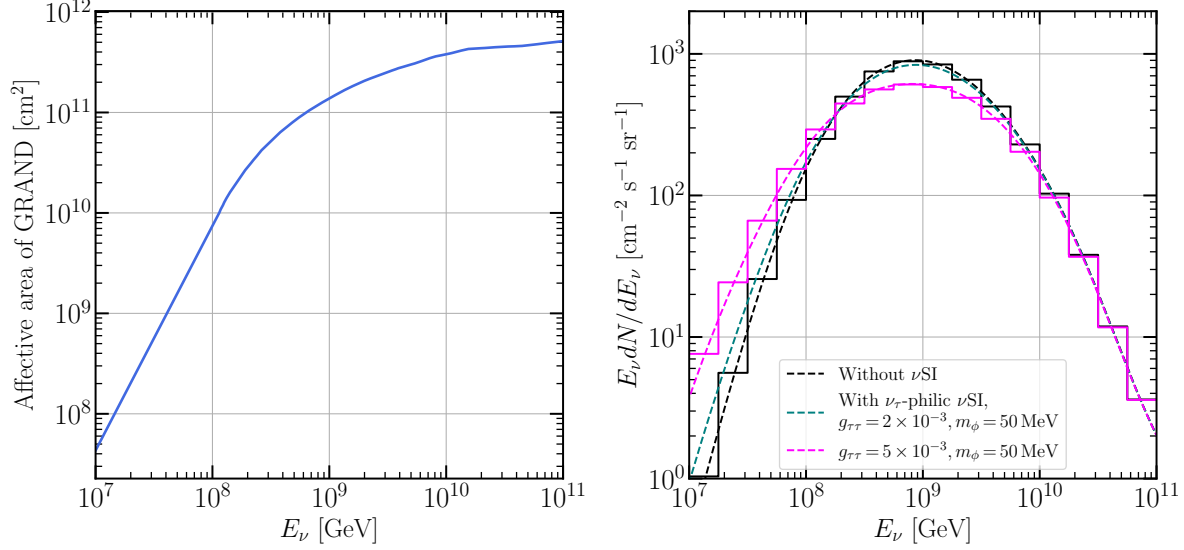


Figure 4: **Left:** direction-averaged effective area of GRAND for UHE tau neutrino detection. **Right:** our calculated event rates of UHE neutrinos at GRAND with ten years of exposure. We also use two histograms to show our energy binning.

To observe the EAS, GRAND aims to measure their radio emission by deploying a large-scale network of up to 200,000 autonomous radio antennas over an area of about 200,000 km<sup>2</sup>, primarily in mountainous regions. We focus on UHE tau neutrinos as the other flavors ( $\nu_e$  and  $\nu_\mu$ ) can hardly produce “Earth-emergent” air showers suitable for observations.

With the direction-averaged effective area,  $A_{\text{eff}}$ , and  $T_{\text{obs}} = 10$  years of exposure, it is straightforward to calculate the event rate by

$$\frac{dN}{dE_\nu} = 4\pi T_{\text{obs}} A_{\text{eff}}(E_\nu) \Phi_{\nu,\tau}(E_\nu). \quad (27)$$

Figure 4 left and right panels show the  $A_{\text{eff}}$  [83] and our calculated event rates, respectively. Within ten years, GRAND is expected to detect hundreds of tau neutrinos above 1 EeV. The spectral distortion across a broad energy range due to relativistic CNB yields greater statistical power and overcomes the potential energy-resolution limitation. Note that the  $A_{\text{eff}}$  should be corrected due to certain SM processes, like the neutrino-nucleus W-boson production [84–88] and final-state radiation [89], the former increases the  $A_{\text{eff}}$  by overall  $\sim 10\%$  while the latter decreases  $A_{\text{eff}}$  by overall  $\sim 15\%$ . However, both effects are much smaller than current uncertainties in the UHE neutrino production so we leave these corrections for future studies<sup>3</sup>

Next, to evaluate the sensitivity of UHE neutrino observation at GRAND to  $\nu\text{SI}$ , we perform a likelihood analysis similar to Ref. [32]. The likelihood function is given by [60]

$$\chi^2(m, \Gamma, E_p^{\text{max}} | g, m_\phi) = 2 \sum_k \left[ N_{\text{st},k} - N_k + N_k \ln \frac{N_k}{N_{\text{st},k}} \right], \quad (28)$$

where  $N_{\text{st},k}$  and  $N_k$  denote the event numbers in the  $k$ -th energy bin in the without and with  $\nu\text{SI}$ , respectively. In our analysis, we marginalize over  $m \in [-3.0, 3.0]$ ,  $\Gamma \in [2.0, 3.0]$ , and  $E_p^{\text{max}} \in [10^2, 10^5]$

<sup>3</sup>Note that for another promising UHE neutrino detection strategy, in-ice radio detectors, final state radiation increases the  $A_{\text{eff}}$  by as much as  $\sim 60\%$  [89], which should be included in the phenomenology studies [89].

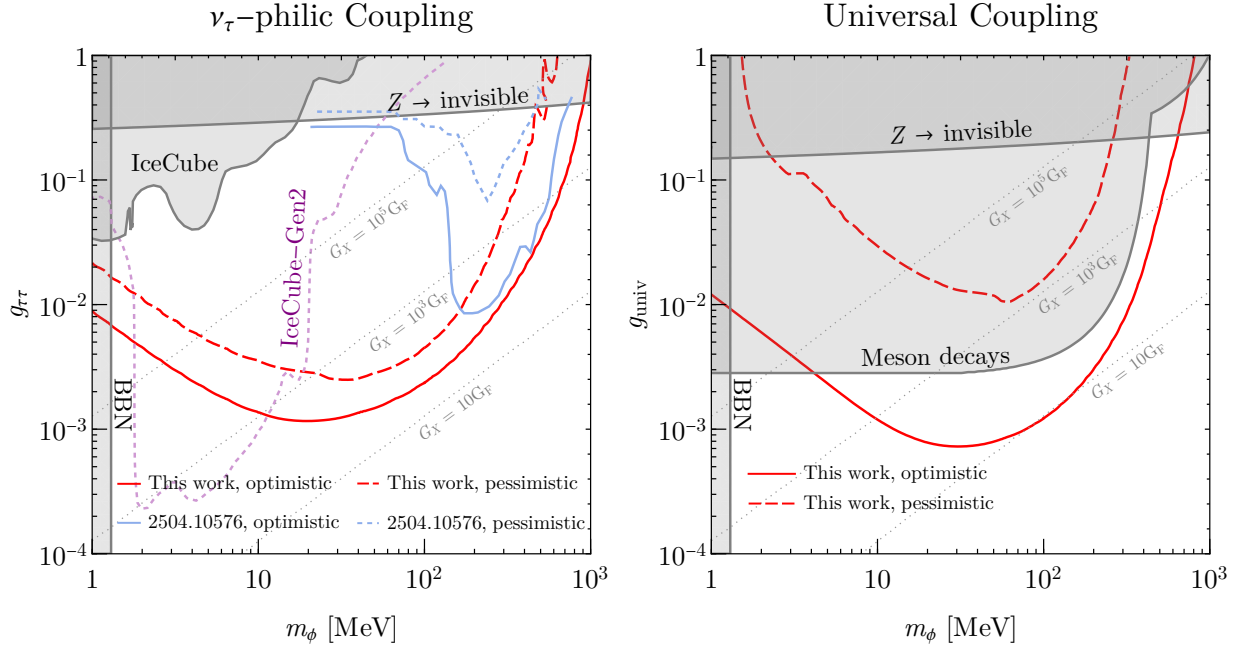


Figure 5: **(Main result of the paper.)** Our projected sensitivities on  $\nu$ SI from UHE neutrinos absorbed by relativistic CNB, i.e., under the “widening the resonance” scenario, along with results from previous works. **Red solid (dashed) curves:** our sensitivities using the GRAND UHE neutrino detector, assuming optimistic (pessimistic) fluxes. **Blue curves:** previous results from UHE neutrinos absorbed by non-relativistic CNB with optimistic (solid) and pessimistic (dashed) fluxes [32]. **Purple dashed curve:** earlier results from HE neutrinos absorbed by relativistic CNB and detected by IceCube-Gen2 (dashed) [18]. **The gray shaded regions** are those excluded by  $Z$  boson invisible decay [4], BBN [3], rare meson decay (universal coupling only) [90], and IceCube HE neutrino observation ( $\nu_\tau$ -philic coupling only) [91].

around two benchmark points, optimistic scenario ( $m = 3$ ) and pessimistic scenario ( $m = 0$ ), both with  $\Gamma = 2.5$ ,  $E_{\max} = 250$  EeV; this encompasses the uncertainties in the cosmogenic UHE neutrino production. We include the parameters  $\lambda$  and  $m$  to account for astrophysical uncertainties in  $N_{\text{st},k}$  and marginalize them in the frequentist treatment [60]. The energy bins are from 0.01 to 100 EeV with logarithmic bin widths  $\log_{10}(E_{\text{high}}/E_{\text{low}}) = 0.25$ , accounting for the energy resolution of GRAND; thus we have 16 bins in total.

Figure 5 shows our projected sensitivities (red curves) alongside experimental or projected constraints from earlier studies. Our result demonstrates that future observations of UHE neutrinos by GRAND can probe  $\nu$ SI with the mediator mass up to 1 GeV and the coupling down to  $10^{-3}$ . For  $\nu_\tau$ -philic coupling, our result surpasses the existing limit from  $Z$  boson invisible decay by two orders of magnitude. For universal coupling, rare meson decays set stringent limits. Our results, however, still surpass the current limits by a factor of a few for mediators heavier than 10 MeV.

Finally, we emphasize the key difference between our work and earlier studies in Refs. [18, 32]. Thanks to the widened resonance arising from relativistic CNB, our sensitivities not only fill the gap between using HE [18] and UHE neutrinos [32] scattering off the non-relativistic CNB, but also cover a significantly broader range of the mediator mass. Comparing with Ref. [32], which studies the case of non-relativistic CNB with the same UHE neutrinos and detection setup, we find that, if the lightest neutrino in the CNB is relativistic, the widened resonance can significantly expand

the sensitivity reach of GRAND. Reference [18] focused on TeV–PeV neutrinos, so the lower-mass regime of  $\nu$ SI was probed. Although not considered in this work, we anticipate that using the same TeV–PeV neutrinos and detection setup as Ref. [18], if there is a relativistic component in the CNB, the widened resonance would expand the sensitivity reach obtained in Ref. [18] as well.

## 6 Conclusion

Cosmic messengers play a central role in probing new physics beyond the standard model. This is because they provide experimental conditions far beyond the reach of laboratory experiments and serve as a link between laboratory discoveries of new fundamental physics and its role in the Universe, where many new physics motivations originate. On the other hand, neutrino self-interactions are well-motivated by nonzero neutrino masses, which typically require introducing new mediators that pass new forces between neutrinos. These  $\nu$ SI have rich phenomena in particle physics, astrophysics, and cosmology, and have been a vibrant subject in recent years.

In this work, we extend the “widening the resonance” concept to ultrahigh-energy neutrinos and probe an uncharted region of parameter space of  $\nu$ SI in the high-mass regime. The incoming UHE neutrinos scatter off the relativistic CNB due to  $\nu$ SI, leading to distortions of the UHE neutrino spectra. The relativistic CNB exhibits a broad spectrum rather than the  $\delta$ -function-like spectrum of the non-relativistic CNB; this broadens the resonance of  $\nu$ SI and significantly enhances the spectral distortion.

Meanwhile, we provide a semi-analytic framework to calculate the cosmogenic UHE neutrino production, avoiding computationally intensive simulations and precise enough for phenomenology studies. This framework, which significantly simplifies the computation, can be directly applied to future phenomenology studies.

We solve the Boltzmann equations that govern the neutrino propagation, which reveal the spectrum distortion. Then, we use GRAND, a future powerful UHE neutrino detector, to probe such distorted spectra. Using proper likelihood analyses, we derive our projected sensitivities. The widened resonance provides key advantages: it affects a wider range of UHE neutrino spectra, yielding greater statistics and overcoming the potential energy-resolution limitation. Our sensitivities with optimistic UHE neutrino fluxes show that GRAND can probe the  $\nu$ SI mediator with MeV–GeV masses with couplings down to  $g \sim 10^{-3}$ , corresponding to  $G_X \sim 10G_F$ . Our sensitivities with pessimistic flux are weaker by a factor of 2–5 in the  $\nu_\tau$ -philic-coupling case and 10–50 in the universal-coupling case. Overall, our sensitivities lead to improvements of up to two orders of magnitude over current constraints, as well as significant gains with respect to the non-relativistic CNB case.

Looking forward, continued experiments with larger effective areas in UHE neutrino detection and improved precision in modeling UHE neutrino production will make UHE neutrinos even sharper tools for probing fundamental physics. The continuous detection of UHE neutrinos will either place our theoretical forecasts under experimental constraints or lead to discovery.

Our work illustrates a novel way of probing  $\nu$ SI. The “widening the resonance” is a general concept when both initial states follow continuum energy distributions. Thus, more phenomenology studies along this direction can be performed.

## Acknowledgement

P.M., I.R.W., and B.Z. are supported by Fermi Forward Discovery Group, LLC under Contract No. 89243024CSC000002 with the U.S. Department of Energy, Office of Science, Office of High Energy Physics. I.R.W. is also supported by DOE distinguished scientist fellowship grant FNAL



22-33. X.J.X is supported in part by the National Natural Science Foundation of China under grant No. 12141501 and also by the CAS Project for Young Scientists in Basic Research (YSBR-099). We are grateful for the computing resources of Rutgers CMS group.

## A More details for Section 3—modeling cosmogenic UHE neutrino production

In this section, following Ref. [72], we provide the necessary details for  $\Psi_i(\eta, x)$  in Eq. (21), which is the neutrino spectrum per proton-photon interaction.

The scattering cross sections of photopion production are determined by the CoM energy, parametrized by  $\eta$ . The kinematics gives a lower bound on  $\eta$ ,

$$\eta \geq \eta_0 \equiv 2 \frac{m_\pi}{m_p} + \frac{m_\pi^2}{m_p} \simeq 0.313. \quad (29)$$

Below this bound,  $\Psi_i = 0$ . We further define  $x_\pm$  related to the maximum and minimum energies of pions,

$$x_\pm \equiv \frac{1}{2(1+\eta)} \left[ \eta + r^2 \pm \sqrt{(\eta - r^2 - 2r)(\eta - r^2 + 2r)} \right], \quad (30)$$

where  $r \equiv m_\pi/m_p \simeq 0.146$ .

Ref. [72] provides an analytic form for  $\Psi_i(\eta, x)$ , which is obtained by fitting their simulated data,

$$\Psi_i(\eta, x) = B_i \exp \left[ -s_i \left( \frac{x}{x'_-} \right)^{\delta_i} \right] \times \left[ \ln \left( \frac{2}{1+y'^2} \right) \right]^{\psi_i}. \quad (31)$$

Here  $i$  stands for the neutrino species.  $B_i$ ,  $s_i$ , and  $\delta_i$  are all functions of  $\eta$ , whose values are provided in Tables II and III of Ref. [72]. The  $y'$  is defined as

$$y' \equiv \frac{x - x'_-}{x'_+ - x'_-}. \quad (32)$$

The  $\psi_i$  and the relation between  $x'_\pm$  and  $x_\pm$  are given species-by-species. We define  $\rho \equiv \eta/\eta_0$  for convenience. The results are summarized as follows, and we refer the readers to Sec. II.B of Ref. [72] for more detailed explanations.

**$\bar{\nu}_\mu$  and  $\nu_e$ :**

$$\psi = 2.5 + 1.4 \ln \rho, \quad x'_- = x_-/4, \quad x'_+ = x_+, \quad (33)$$

**$\nu_\mu$ :**

$$\begin{aligned} \psi &= 2.5 + 1.4 \ln(\rho), \quad x'_- = 0.427x_-, \\ x'_+ &= \begin{cases} 0.427x_+, & \rho < 2.14, \\ x_+ (0.427 + 0.0729(\rho - 2.14)), & 2.14 < \rho < 10, \\ x_+, & \rho > 10. \end{cases} \end{aligned} \quad (34)$$

**$\bar{\nu}_e$ :** The form for this flavor is different from others, as  $\pi^+$  cannot produce  $\bar{\nu}_e$  via its decay so that an additional  $\pi^-$  needs to be produced simultaneously. This requires

$$\eta > 4r(1+r) \simeq 2.14\eta_0. \quad (35)$$

The definition of  $x_{\pm}$  for  $\bar{\nu}_e$  is

$$x_{\pm} \equiv \frac{1}{2(1+\eta)} \left( \eta - 2r \pm \sqrt{\eta(\eta - 4r(1+r))} \right). \quad (36)$$

The other quantities needed in Eq. (31) is given by

$$\psi = 6 \left( 1 - e^{1.5(4-\rho)} \right) \Theta(\rho - 4), \quad x'_- = x_-/2, \quad x'_+ = x_+, \quad (37)$$

where  $\Theta$  is the Heaviside function.

## References

- [1] I. R. Wang, X.-J. Xu, and B. Zhou, “Widen the Resonance: Probing a New Regime of Neutrino Self-Interactions with Astrophysical Neutrinos,” *Phys. Rev. Lett.* **135** (2025) 181002, [arXiv:2501.07624 \[hep-ph\]](#).
- [2] C. D. Kreisch, F.-Y. Cyr-Racine, and O. Doré, “Neutrino puzzle: Anomalies, interactions, and cosmological tensions,” *Phys. Rev. D* **101** (2020) no. 12, 123505, [arXiv:1902.00534 \[astro-ph.CO\]](#).
- [3] N. Blinov, K. J. Kelly, G. Z. Krnjaic, and S. D. McDermott, “Constraining the Self-Interacting Neutrino Interpretation of the Hubble Tension,” *Phys. Rev. Lett.* **123** (2019) no. 19, 191102, [arXiv:1905.02727 \[astro-ph.CO\]](#).
- [4] V. Brdar, M. Lindner, S. Vogl, and X.-J. Xu, “Revisiting neutrino self-interaction constraints from  $Z$  and  $\tau$  decays,” *Phys. Rev. D* **101** (2020) no. 11, 115001, [arXiv:2003.05339 \[hep-ph\]](#).
- [5] F. F. Deppisch, L. Graf, W. Rodejohann, and X.-J. Xu, “Neutrino Self-Interactions and Double Beta Decay,” *Phys. Rev. D* **102** (2020) no. 5, 051701, [arXiv:2004.11919 \[hep-ph\]](#).
- [6] S. Roy Choudhury, S. Hannestad, and T. Tram, “Updated constraints on massive neutrino self-interactions from cosmology in light of the  $H_0$  tension,” *JCAP* **03** (2021) 084, [arXiv:2012.07519 \[astro-ph.CO\]](#).
- [7] S. Roy Choudhury, S. Hannestad, and T. Tram, “Massive neutrino self-interactions and inflation,” *JCAP* **10** (2022) 018, [arXiv:2207.07142 \[astro-ph.CO\]](#).
- [8] J. Venzor, G. Garcia-Arroyo, J. De-Santiago, and A. Pérez-Lorezana, “Resonant neutrino self-interactions and the  $H_0$  tension,” *Phys. Rev. D* **108** (2023) no. 4, 043536, [arXiv:2303.12792 \[astro-ph.CO\]](#).
- [9] A. Das, A. Dighe, and M. Sen, “New effects of non-standard self-interactions of neutrinos in a supernova,” *JCAP* **05** (2017) 051, [arXiv:1705.00468 \[hep-ph\]](#).
- [10] S. Shalgar, I. Tamborra, and M. Bustamante, “Core-collapse supernovae stymie secret neutrino interactions,” *Phys. Rev. D* **103** (2021) no. 12, 123008, [arXiv:1912.09115 \[astro-ph.HE\]](#).
- [11] P.-W. Chang, I. Esteban, J. F. Beacom, T. A. Thompson, and C. M. Hirata, “Toward Powerful Probes of Neutrino Self-Interactions in Supernovae,” *Phys. Rev. Lett.* **131** (2023) no. 7, 071002, [arXiv:2206.12426 \[hep-ph\]](#).
- [12] D. F. G. Fiorillo, G. G. Raffelt, and E. Vitagliano, “Large Neutrino Secret Interactions Have a Small Impact on Supernovae,” *Phys. Rev. Lett.* **132** (2024) no. 2, 021002, [arXiv:2307.15115 \[hep-ph\]](#).
- [13] D. F. G. Fiorillo, G. G. Raffelt, and E. Vitagliano, “Supernova emission of secretly interacting neutrino fluid: Theoretical foundations,” *Phys. Rev. D* **109** (2024) no. 2, 023017, [arXiv:2307.15122 \[hep-ph\]](#).

- [14] Q.-f. Wu and X.-J. Xu, “Shedding light on neutrino self-interactions with solar antineutrino searches,” *JCAP* **02** (2024) 037, [arXiv:2308.15849 \[hep-ph\]](#).
- [15] K. C. Y. Ng and J. F. Beacom, “Cosmic neutrino cascades from secret neutrino interactions,” *Phys. Rev. D* **90** (2014) no. 6, 065035, [arXiv:1404.2288 \[astro-ph.HE\]](#). [Erratum: *Phys. Rev. D* **90**, 089904 (2014)].
- [16] K. Ioka and K. Murase, “IceCube PeV–EeV neutrinos and secret interactions of neutrinos,” *PTEP* **2014** (2014) no. 6, 061E01, [arXiv:1404.2279 \[astro-ph.HE\]](#).
- [17] M. Bustamante, C. Rosenstrøm, S. Shalgar, and I. Tamborra, “Bounds on secret neutrino interactions from high-energy astrophysical neutrinos,” *Phys. Rev. D* **101** (2020) no. 12, 123024, [arXiv:2001.04994 \[astro-ph.HE\]](#).
- [18] I. Esteban, S. Pandey, V. Brdar, and J. F. Beacom, “Probing secret interactions of astrophysical neutrinos in the high-statistics era,” *Phys. Rev. D* **104** (2021) no. 12, 123014, [arXiv:2107.13568 \[hep-ph\]](#).
- [19] C. Creque-Sarbinowski, J. Hyde, and M. Kamionkowski, “Resonant neutrino self-interactions,” *Phys. Rev. D* **103** (2021) no. 2, 023527, [arXiv:2005.05332 \[hep-ph\]](#).
- [20] A. Das, Y. F. Perez-Gonzalez, and M. Sen, “Neutrino secret self-interactions: A booster shot for the cosmic neutrino background,” *Phys. Rev. D* **106** (2022) no. 9, 095042, [arXiv:2204.11885 \[hep-ph\]](#).
- [21] K. Akita, S. H. Im, and M. Masud, “Probing non-standard neutrino interactions with a light boson from next galactic and diffuse supernova neutrinos,” *JHEP* **12** (2022) 050, [arXiv:2206.06852 \[hep-ph\]](#).
- [22] A. B. Balantekin, G. M. Fuller, A. Ray, and A. M. Suliga, “Probing self-interacting sterile neutrino dark matter with the diffuse supernova neutrino background,” *Phys. Rev. D* **108** (2023) no. 12, 123011, [arXiv:2310.07145 \[hep-ph\]](#).
- [23] C. Döring and S. Vogl, “Testing secret interaction with astrophysical neutrino point sources,” *JCAP* **07** (2024) 015, [arXiv:2304.08533 \[hep-ph\]](#).
- [24] X. Luo, W. Rodejohann, and X.-J. Xu, “Dirac neutrinos and  $N_{\text{eff}}$ ,” *JCAP* **06** (2020) 058, [arXiv:2005.01629 \[hep-ph\]](#).
- [25] G.-y. Huang, T. Ohlsson, and S. Zhou, “Observational Constraints on Secret Neutrino Interactions from Big Bang Nucleosynthesis,” *Phys. Rev. D* **97** (2018) no. 7, 075009, [arXiv:1712.04792 \[hep-ph\]](#).
- [26] X. Chu, B. Dasgupta, M. Dentler, J. Kopp, and N. Saviano, “Sterile neutrinos with secret interactions—cosmological discord?,” *JCAP* **11** (2018) 049, [arXiv:1806.10629 \[hep-ph\]](#).
- [27] E. Grohs, G. M. Fuller, and M. Sen, “Consequences of neutrino self interactions for weak decoupling and big bang nucleosynthesis,” *JCAP* **07** (2020) 001, [arXiv:2002.08557 \[astro-ph.CO\]](#).
- [28] S.-P. Li and X.-J. Xu, “ $N_{\text{eff}}$  constraints on light mediators coupled to neutrinos: the dilution-resistant effect,” *JHEP* **10** (2023) 012, [arXiv:2307.13967 \[hep-ph\]](#).
- [29] I. R. Wang and X.-J. Xu, “Imprints of light dark matter on the evolution of cosmic neutrinos,” *JCAP* **05** (2024) 050, [arXiv:2312.17151 \[hep-ph\]](#).
- [30] D. E. Kaplan, X. Luo, and S. Rajendran, “Probing Long-Range Forces Between Neutrinos with Cosmic Structures,” [arXiv:2412.20766 \[hep-ph\]](#).
- [31] Y. He, J. Liu, X.-P. Wang, and Y.-M. Zhong, “Implications of the KM3NeT Ultrahigh-energy Event on Neutrino Self-interactions,” [arXiv:2504.20163 \[hep-ph\]](#).
- [32] L. P. S. Leal, D. Naredo-Tuero, and R. Z. Funchal, “Cosmogenic neutrinos as probes of new physics,” *JHEP* **08** (2025) 057, [arXiv:2504.10576 \[hep-ph\]](#).

- [33] A. Poudou, T. Simon, T. Montandon, E. M. Teixeira, and V. Poulin, “Self-interacting neutrinos in light of recent CMB and LSS data,” *Phys. Rev. D* **112** (2025) no. 10, 103535, [arXiv:2503.10485 \[astro-ph.CO\]](#).
- [34] J. M. Berryman *et al.*, “Neutrino self-interactions: A white paper,” *Phys. Dark Univ.* **42** (2023) 101267, [arXiv:2203.01955 \[hep-ph\]](#).
- [35] M. Ackermann *et al.*, “High-energy and ultra-high-energy neutrinos: A Snowmass white paper,” *JHEAp* **36** (2022) 55–110, [arXiv:2203.08096 \[hep-ph\]](#).
- [36] Y. Bai, K. Xie, and B. Zhou, “Large Neutrino ”Collider”,” [arXiv:2510.13948 \[hep-ph\]](#).
- [37] Y. Chikashige, R. N. Mohapatra, and R. D. Peccei, “Are There Real Goldstone Bosons Associated with Broken Lepton Number?,” *Phys. Lett. B* **98** (1981) 265–268.
- [38] G. B. Gelmini and M. Roncadelli, “Left-Handed Neutrino Mass Scale and Spontaneously Broken Lepton Number,” *Phys. Lett. B* **99** (1981) 411–415.
- [39] C. S. Aulakh and R. N. Mohapatra, “Neutrino as the Supersymmetric Partner of the Majoron,” *Phys. Lett. B* **119** (1982) 136–140.
- [40] X.-G. He, G. C. Joshi, H. Lew, and R. R. Volkas, “Simplest Z-prime model,” *Phys. Rev. D* **44** (1991) 2118–2132.
- [41] E. Salvioni, A. Strumia, G. Villadoro, and F. Zwirner, “Non-universal minimal Z’ models: present bounds and early LHC reach,” *JHEP* **03** (2010) 010, [arXiv:0911.1450 \[hep-ph\]](#).
- [42] M. Lindner, D. Schmidt, and A. Watanabe, “Dark matter and U(1)’ symmetry for the right-handed neutrinos,” *Phys. Rev. D* **89** (2014) no. 1, 013007, [arXiv:1310.6582 \[hep-ph\]](#).
- [43] E. Ma, I. Picek, and B. Radovčić, “New Scotogenic Model of Neutrino Mass with  $U(1)_D$  Gauge Interaction,” *Phys. Lett. B* **726** (2013) 744–746, [arXiv:1308.5313 \[hep-ph\]](#).
- [44] E. Bertuzzo, P. A. N. Machado, Z. Tabrizi, and R. Zukanovich Funchal, “A Neutrophilic 2HDM as a UV Completion for the Inverse Seesaw Mechanism,” *JHEP* **11** (2017) 004, [arXiv:1706.10000 \[hep-ph\]](#).
- [45] K. S. Babu, A. Friedland, P. A. N. Machado, and I. Mocioiu, “Flavor Gauge Models Below the Fermi Scale,” *JHEP* **12** (2017) 096, [arXiv:1705.01822 \[hep-ph\]](#).
- [46] M. Berbig, S. Jana, and A. Trautner, “The Hubble tension and a renormalizable model of gauged neutrino self-interactions,” *Phys. Rev. D* **102** (2020) no. 11, 115008, [arXiv:2004.13039 \[hep-ph\]](#).
- [47] X.-J. Xu, “The  $\nu_R$ -philic scalar: its loop-induced interactions and Yukawa forces in LIGO observations,” *JHEP* **09** (2020) 105, [arXiv:2007.01893 \[hep-ph\]](#).
- [48] G. Chauhan and X.-J. Xu, “How dark is the  $\nu_R$ -philic dark photon?,” *JHEP* **04** (2021) 003, [arXiv:2012.09980 \[hep-ph\]](#).
- [49] S. Foroughi-Abari, K. J. Kelly, M. Rai, and Y. Zhang, “Enabling Strong Neutrino Self-Interaction with an Unparticle Mediator,” *Phys. Rev. Lett.* **134** (2025) no. 18, 181001, [arXiv:2501.02049 \[hep-ph\]](#).
- [50] K. J. Kelly and P. A. N. Machado, “Multimessenger Astronomy and New Neutrino Physics,” *JCAP* **10** (2018) 048, [arXiv:1808.02889 \[hep-ph\]](#).
- [51] K. J. Kelly, M. Sen, W. Tangarife, and Y. Zhang, “Origin of sterile neutrino dark matter via secret neutrino interactions with vector bosons,” *Phys. Rev. D* **101** (2020) no. 11, 115031, [arXiv:2005.03681 \[hep-ph\]](#).
- [52] K. S. Babu, “Model of ’Calculable’ Majorana Neutrino Masses,” *Phys. Lett. B* **203** (1988) 132–136.

- [53] A. Abada, S. Davidson, A. Ibarra, F. X. Josse-Michaux, M. Losada, and A. Riotto, “Flavour Matters in Leptogenesis,” *JHEP* **09** (2006) 010, [arXiv:hep-ph/0605281](#).
- [54] A. Abada and M. Lucente, “Looking for the minimal inverse seesaw realisation,” *Nucl. Phys. B* **885** (2014) 651–678, [arXiv:1401.1507 \[hep-ph\]](#).
- [55] **DESI** Collaboration, A. G. Adame *et al.*, “DESI 2024 VI: cosmological constraints from the measurements of baryon acoustic oscillations,” *JCAP* **02** (2025) 021, [arXiv:2404.03002 \[astro-ph.CO\]](#).
- [56] J. F. Beacom, “The Diffuse Supernova Neutrino Background,” *Ann. Rev. Nucl. Part. Sci.* **60** (2010) 439–462, [arXiv:1004.3311 \[astro-ph.HE\]](#).
- [57] I. Esteban, M. C. Gonzalez-Garcia, M. Maltoni, T. Schwetz, and A. Zhou, “The fate of hints: updated global analysis of three-flavor neutrino oscillations,” *JHEP* **09** (2020) 178, [arXiv:2007.14792 \[hep-ph\]](#).
- [58] <http://www.nu-fit.org/>.
- [59] T. M. P. Tait, “TASI Lectures on Resonances,” 2009. [www.physics.uci.edu/~ttait/tait-TASI08.pdf](http://www.physics.uci.edu/~ttait/tait-TASI08.pdf).
- [60] **Particle Data Group** Collaboration, S. Navas *et al.*, “Review of particle physics,” *Phys. Rev. D* **110** (2024) no. 3, 030001.
- [61] M. S. Muzio, “Ultrahigh energy cosmic rays and neutrino flux models,” *Eur. Phys. J. ST* **234** (2025) no. 16, 4939–4949, [arXiv:2502.11834 \[astro-ph.HE\]](#).
- [62] N. Senno, K. Murase, and P. Meszaros, “Choked Jets and Low-Luminosity Gamma-Ray Bursts as Hidden Neutrino Sources,” *Phys. Rev. D* **93** (2016) no. 8, 083003, [arXiv:1512.08513 \[astro-ph.HE\]](#).
- [63] P.-W. Chang, B. Zhou, K. Murase, and M. Kamionkowski, “High-energy neutrinos from choked-jet supernovae: Searches and implications,” *Phys. Rev. D* **109** (2024) no. 10, 103041, [arXiv:2210.03088 \[astro-ph.HE\]](#).
- [64] S. W. Li, P. Machado, D. Naredo-Tuero, and T. Schwemberger, “Clash of the Titans: ultra-high energy KM3NeT event versus IceCube data,” [arXiv:2502.04508 \[astro-ph.HE\]](#).
- [65] **KM3NeT** Collaboration, S. Aiello *et al.*, “Observation of an ultra-high-energy cosmic neutrino with KM3NeT,” *Nature* **638** (2025) no. 8050, 376–382. [Erratum: *Nature* 640, E3 (2025)].
- [66] K. Møller, P. B. Denton, and I. Tamborra, “Cosmogenic Neutrinos Through the GRAND Lens Unveil the Nature of Cosmic Accelerators,” *JCAP* **05** (2019) 047, [arXiv:1809.04866 \[astro-ph.HE\]](#).
- [67] H. Yuksel, M. D. Kistler, J. F. Beacom, and A. M. Hopkins, “Revealing the High-Redshift Star Formation Rate with Gamma-Ray Bursts,” *Astrophys. J. Lett.* **683** (2008) L5–L8, [arXiv:0804.4008 \[astro-ph\]](#).
- [68] M. Ajello *et al.*, “The Cosmic Evolution of Fermi BL Lacertae Objects,” *Astrophys. J.* **780** (2014) 73, [arXiv:1310.0006 \[astro-ph.CO\]](#).
- [69] P. Padovani, M. Petropoulou, P. Giommi, and E. Resconi, “A simplified view of blazars: the neutrino background,” *Mon. Not. Roy. Astron. Soc.* **452** (2015) no. 2, 1877–1887, [arXiv:1506.09135 \[astro-ph.HE\]](#).
- [70] M. Petropoulou, D. Giannios, and L. Sironi, “Blazar flares powered by plasmoids in relativistic reconnection,” *Mon. Not. Roy. Astron. Soc.* **462** (2016) no. 3, 3325–3343, [arXiv:1606.07447 \[astro-ph.HE\]](#).

- [71] Y. Qu, H. Zeng, and D. Yan, “Gamma-ray luminosity function of BL Lac objects and contribution to the extragalactic gamma-ray background,” *Mon. Not. Roy. Astron. Soc.* **490** (2019) no. 1, 758–765, [arXiv:1909.07542 \[astro-ph.HE\]](#).
- [72] S. R. Kelner and F. A. Aharonian, “Energy spectra of gamma-rays, electrons and neutrinos produced at interactions of relativistic protons with low energy radiation,” *Phys. Rev. D* **78** (2008) 034013, [arXiv:0803.0688 \[astro-ph\]](#). [Erratum: *Phys.Rev.D* 82, 099901 (2010)].
- [73] A. van Vliet, R. Alves Batista, and J. R. Hörandel, “Determining the fraction of cosmic-ray protons at ultrahigh energies with cosmogenic neutrinos,” *Phys. Rev. D* **100** (2019) no. 2, 021302, [arXiv:1901.01899 \[astro-ph.HE\]](#).
- [74] V. S. Berezinsky and G. T. Zatsepin, “Cosmic rays at ultrahigh-energies (neutrino?),” *Phys. Lett. B* **28** (1969) 423–424.
- [75] K. Kotera, D. Allard, and A. V. Olinto, “Cosmogenic Neutrinos: parameter space and detectability from PeV to ZeV,” *JCAP* **10** (2010) 013, [arXiv:1009.1382 \[astro-ph.HE\]](#).
- [76] R. Aloisio, D. Boncioli, A. di Matteo, A. F. Grillo, S. Petrera, and F. Salamida, “Cosmogenic neutrinos and ultra-high energy cosmic ray models,” *JCAP* **10** (2015) 006, [arXiv:1505.04020 \[astro-ph.HE\]](#).
- [77] **CRPropa** Collaboration, R. Alves Batista, A. Dundovic, M. Erdmann, K.-H. Kampert, D. Kuempel, G. Müller, G. Sigl, A. van Vliet, D. Walz, and T. Winchen, “CRPropa 3 - a Public Astrophysical Simulation Framework for Propagating Extraterrestrial Ultra-High Energy Particles,” *JCAP* **05** (2016) 038, [arXiv:1603.07142 \[astro-ph.IM\]](#).
- [78] G. R. Blumenthal, “Energy loss of high-energy cosmic rays in pair-producing collisions with ambient photons,” *Phys. Rev. D* **1** (1970) 1596–1602.
- [79] V. S. Berezinsky and S. I. Grigor’eva, “A Bump in the ultrahigh-energy cosmic ray spectrum,” *Astron. Astrophys.* **199** (1988) 1–12.
- [80] **Pierre Auger** Collaboration, A. Aab *et al.*, “Measurement of the cosmic-ray energy spectrum above  $2.5 \times 10^{18}$  eV using the Pierre Auger Observatory,” *Phys. Rev. D* **102** (2020) no. 6, 062005, [arXiv:2008.06486 \[astro-ph.HE\]](#).
- [81] **Pierre Auger** Collaboration, F. Fenu, “The cosmic ray energy spectrum measured with the Pierre Auger Observatory,” *Adv. Space Res.* **72** (2023) 3531–3537.
- [82] R. Alves Batista, D. Boncioli, A. di Matteo, and A. van Vliet, “Secondary neutrino and gamma-ray fluxes from SimProp and CRPropa,” *JCAP* **05** (2019) 006, [arXiv:1901.01244 \[astro-ph.HE\]](#).
- [83] **GRAND** Collaboration, J. Álvarez-Muñoz *et al.*, “The Giant Radio Array for Neutrino Detection (GRAND): Science and Design,” *Sci. China Phys. Mech. Astron.* **63** (2020) no. 1, 219501, [arXiv:1810.09994 \[astro-ph.HE\]](#).
- [84] D. Seckel, “Neutrino photon reactions in astrophysics and cosmology,” *Phys. Rev. Lett.* **80** (1998) 900–903, [arXiv:hep-ph/9709290](#).
- [85] I. Alikhanov, “Hidden Glashow resonance in neutrino–nucleus collisions,” *Phys. Lett. B* **756** (2016) 247–253, [arXiv:1503.08817 \[hep-ph\]](#).
- [86] B. Zhou and J. F. Beacom, “W-boson and trident production in TeV–PeV neutrino observatories,” *Phys. Rev. D* **101** (2020) no. 3, 036010, [arXiv:1910.10720 \[hep-ph\]](#).
- [87] B. Zhou and J. F. Beacom, “Neutrino-nucleus cross sections for W-boson and trident production,” *Phys. Rev. D* **101** (2020) no. 3, 036011, [arXiv:1910.08090 \[hep-ph\]](#).
- [88] **CTEQ-TEA** Collaboration, K. Xie, B. Zhou, and T. J. Hobbs, “The photon content of the neutron,” *JHEP* **04** (2024) 022, [arXiv:2305.10497 \[hep-ph\]](#).

- [89] R. Plestid and B. Zhou, “Final state radiation from high and ultrahigh energy neutrino interactions,” *Phys. Rev. D* **111** (2025) no. 4, 043007, [arXiv:2403.07984 \[hep-ph\]](#).
- [90] J. M. Berryman, A. De Gouvêa, K. J. Kelly, and Y. Zhang, “Lepton-Number-Charged Scalars and Neutrino Beamstrahlung,” *Phys. Rev. D* **97** (2018) no. 7, 075030, [arXiv:1802.00009 \[hep-ph\]](#).
- [91] **IceCube** Collaboration, R. Abbasi *et al.*, “The IceCube high-energy starting event sample: Description and flux characterization with 7.5 years of data,” *Phys. Rev. D* **104** (2021) 022002, [arXiv:2011.03545 \[astro-ph.HE\]](#).